High export of nitrogen and dissolved organic carbon from an Alpine glacier (Indren Glacier, NW Italian Alps)

High export of nitrogen and dissolved organic carbon from an Alpine glacier (Indren Glacier, NW Italian Alps)

Nicola Colombo[1,5*], Daniele Bocchiola[2,5], Maria Martin[1], Gabriele Confortola[2], Franco Salerno[3], Danilo Godone[4,5], Michele D'Amico[1], Michele Freppaz[1,5]

[1]University of Turin, Department of Agricultural, Forest and Food Sciences, Largo Paolo Braccini, 2, 10095, Grugliasco, Italy

[2]Politecnico di Milano, Department of Civil and Environmental Engineering, Piazza Leonardo da Vinci, 32, 20133, Milano, Italy

[3]CNR-IRSA (National Research Council - Water Research Institute), Via del Mulino, 19, 20047, Brugherio, Italy

[4]CNR-IRPI (National Research Council - Research Institute for Geo-Hydrological Protection), Strada delle Cacce, 73, 10135, Turin, Italy

[5]University of Turin, Research Center on Natural Risk in Mountain and Hilly Environments, NatRisk, Largo Paolo Braccini, 2, 10095, Grugliasco, Italy

[*]*Correspondence to*: nicola.colombo@unito.it

Abstract

Mountain glaciers can export large amounts of nitrogen (N) and carbon (C) to downstream aquatic ecosystems. To date, however, the number of studies that analysed concentrations and fluxes of N forms and dissolved organic carbon (DOC) from glaciers in the European Alps and worldwide is limited, given the high complexity of data gathering in harsh high-elevation environments. In this work, we rely upon new, unexploited data from field campaigns pursued during 2012–2015 at high elevations (> 3000 m a.s.l.) of the Indren Glacier (NW Italian Alps) to i) develop glacio-hydrological modelling and stream flow estimates within a heavily glacier-fed catchment, ii) provide N forms and DOC concentrations and estimated fluxes in meltwater, and iii) provide possible explanations of cryospheric control upon water chemistry. Water and soil samples were also collected at two lower-elevation sites along the glacial stream to investigate the downstream variability of N forms and DOC. Nitrate-N, dissolved organic nitrogen (DON), and DOC concentrations (0.21 ± 0.12, 0.19 ± 0.14, 1.16 ± 0.63 mg L^{-1}, respectively) and yields (220, 210, 1,279 kg km^{-2} yr^{-1}, respectively) were among the highest considering other glaciated areas of the globe, probably due to high atmospheric N and C depositions. Limited effect of soil on water characteristics was found and attributed to the reduced soil development in recently deglaciated areas (after the Little Ice Age), thus underlining the role of glacier melting in determining N and C dynamics in high-elevation, Alpine surface waters.

Keywords: Glacier, Dissolved Organic Carbon, Nitrogen, Nitrate, Water chemistry, Soil

1 Introduction

Runoff from glaciated catchments in mountain regions is an important fresh water resource to downstream areas (Viviroli et al. 2011). Modifications in the glacier storage capacity due to climate change can affect the hydrological cycle (Stahl et al. 2008), and these modifications are expected to affect nitrogen (N) and carbon (C) dynamics in glacial meltwaters (Hood et al. 2015; Milner et al. 2017). Overall, glacier melting and associated changes in habitat conditions, such as channel stability, turbidity, temperature, nutrient loadings, and concentrations of legacy pollutants and trace elements can result in complex ecological modifications in mountain waters (Brighenti et al. 2019). The degree of these effects varies depending on the type and size of the glacier, but even mountain glaciers covering a small proportion of watershed can influence water biogeochemistry and ecosystems (Slemmons et al. 2013).

Glacier runoff can act as N source (Milner et al. 2017), concentrated in glacier ice from the atmosphere (Daly and Wania 2005), and originating from microbial ecosystems on and beneath the ice (Wadham et al. 2016). Lakes and streams fed by mountain glaciers have been reported to be enriched in nitrate in comparison to snow/groundwater-fed surface waters (Baron et al. 2009; Slemmons et al. 2017). Several non-mutually exclusive factors (Slemmons et al. 2017) could explain the N enrichment of glacier meltwaters such as enhanced nitrification in subglacial environments (Wynn et al. 2007), reduced contact with watershed soils (Brooks et al. 1996), and release through abrasion of old organic N bound in rock (Boyd et al. 2011). Multiple effects of N-enriched glacial meltwater include increased lake primary production (Slemmons and Saros 2012), altered species richness of algal groups (Saros et al. 2010), and modified phytoplankton species composition (Slemmons et al. 2017).

Glaciers have been recently recognised as unique ecosystems with potential implications for the global carbon cycle (Hood et al. 2015). Organic carbon (OC) in glaciers originates from recent and past incorporation into the glacial system (Stubbins et al. 2012; Spencer et al. 2014), accumulating from in situ primary production (Hood et al. 2009; Bhatia et al. 2013), and allochthonous terrestrial (Singer et al. 2012) and anthropogenic (Spencer et al. 2014) sources. Globally, mountain glaciers have been estimated to release approximately 0.8 Tera g yr^{-1} of dissolved organic carbon (DOC) to downstream ecosystems (Li et al. 2018) and the glacier shrinkage can lead to an increase of DOC fluxes reaching downstream ecosystems (Hood et al. 2015). Recent studies have shown that glacier DOC is biologically available, providing a subsidy of bioavailable C to receiving surface waters (Hood et al. 2009; Singer et al. 2012) and sustaining aquatic foodwebs (Fellman et al. 2015).

Although it is clear now that glaciers can be fundamental factors in influencing N and C dynamics in surface waters, few studies have been performed on concentrations and fluxes of major N forms (i.e. nitrate and dissolved organic nitrogen) and DOC from mountain glaciers across the globe (e.g. Lafrenière and Sharp 2005; Baron et al. 2009; Li et al. 2018), and even fewer in the European Alps (e.g. Tockner et al. 2002; Singer et al. 2012). In this work, seasonal time

series of N forms and DOC concentrations and fluxes in the glacial stream originating from the Indren Glacier (NW Italian Alps) are presented. Meltwater samples were collected in the period 2012–2015 and modelled glacier discharge was used to elucidate the role of glacial hydrology on N and C export. Water and soil samples were also collected in the period 2012–2014 at two lower-elevation sites along the glacial stream in order to investigate the downstream variability of N forms and DOC in glacial meltwater.

2 Materials and methods

2.1 Study area

The Indren glacier is a temperate, wet-based mountain glacier (Maggioni et al. 2009), located in the NW Italian Alps, in the Valle d'Aosta Region (Fig. 1), within the LTER (Long term Ecological Research) site, Istituto Mosso. The glacier is in direct contact with a proglacial pond. The glacial stream originates from outflow thereby, and a hydrological station was installed to measure hydrological fluxes (Q1 site, Fig. 1, Tab. 1). The size of the Indren glacier has reduced substantially in the last ~century, retreating by ca. 500 m in the period 1927–2013 (Piccini 2007; Baroni et al. 2014) and loosing ca. 45% of the surface area between 1955 and 2006 (from 1.68 to 0.92 km^2) (CGI-CNR 1961). Strong glacier recession rates have been reported in other areas of the NW Italian Alps due to the impact of climate change (Giaccone et al., 2015; Colombo et al. 2016a; 2016b). According to the long-term climate series (1928–2013) of the Gressoney-La-Trinité - Lago Gabiet automatic weather station (AWS) (2379 m a.s.l., located ca. 4 km far from the Indren glacier, Tab. S1), in the last ~century maximum air temperatures and number of rainy days significantly increased (+0.015 °C $year^{-1}$ and +0.17 days $year^{-1}$, respectively), while fresh snow showed a strong negative trend, although not significant (–1.750 cm $year^{-1}$) (Fratianni et al., 2015). For the 2012–2015 period, the Gabiet AWS recorded a mean air temperature of +2.8 °C, yearly cumulated precipitation (including snow water equivalent) of 1052 mm, and snow thickness of 102 cm. Geologically, the study area is dominated by paraschists, with subordinate leucocratic gneisses, metabasites, metagranites, micaschists, and minor bodies of calcschists and marbles.

2.2 Modelled and measured hydrological flows

A semi-distributed elevation-belt based version of the *Poly-Hydro* model (Soncini et al. 2017), able to reproduce ice and snow dynamics, evapotranspiration, recharge of groundwater reservoir, discharge formation and routing to the control section, was implemented and tuned (Groppelli et al. 2011; Soncini et al. 2015) (further details in Supporting Information (S), Materials and Methods S1.1). Input data to the model are a digital terrain model-DTM, daily values of precipitation and temperature (and their vertical gradient), and land cover information. In this work, a 2x2m-cell DTM and four AWSs close to the glacier were used (Tab. S1, Materials and Methods S1.1).

Poly-Hydro tracks the variation of the water content in the ground within one belt W (mm) in two consecutive time steps (t, $t+\Delta t$), as

$$W^{t+\Delta t} = W^t + R\Delta t + M_s\Delta t + M_i\Delta t - ET\Delta t - Q_g\Delta t \quad (1)$$

here using the daily time step, R = liquid rain, M_s = snowmelt, M_i = ice melt, ET = actual evapotranspiration, and Q_g = groundwater discharge, with all parameters expressed in mm d^{-1}. Overland flow Q_s occurs for saturated soil

$$Q_s = \begin{cases} W^{t+\Delta t} - W_{Max} & if\ W^{t+\Delta t} > W_{Max} \\ 0 & if\ W^{t+\Delta t} \leq W_{Max} \end{cases} \quad (2)$$

with W_{Max} (mm) greatest potential soil storage. Potential evapotranspiration, however small at this high elevation is calculated via Hargreaves equation, requiring temperature data (Bocchiola et al. 2010). Groundwater discharge is a function of soil hydraulic conductivity and water content

$$Q_s = K\left(\frac{W}{W_{Max}}\right)^k \quad (3)$$

with K (mm d^{-1}) saturated permeability and k power exponent.

To depict actual flow variability of this highly glaciated catchment, and to properly tune *Poly-Hydro* model, a flow gauging station was installed downstream of the proglacial pond, at 3083 m a.s.l. (Fig. 1) in 2012 and 2013. The pond outlet was surveyed and modelled as a free surface weir, with outlet coefficient calibrated against flow measures, pursued with a Flow-Tracker® 3D Doppler velocimeter, once per year. Access to the site and operation of the station was possible in safe conditions during short periods (July 19th–October 31st 2012, and July 24th–September 9th in 2013), and the station was shut down in winter. The model outputs were tuned against the observed discharges in these periods.

2.3 Water and soil sampling, and laboratory analyses

Water samples were collected weekly to monthly during the melting seasons 2012–2015 at the pond outlet (W1 site) (Fig. 1, Tab.1). In the period 2012–2014 water samples were also collected at two lower-elevation sites along the glacial stream (W2 and W3 sites) (Fig. 1, Tab.1), selected to describe typical and representative features of the different pedological conditions around the stream, with vegetated soil cover becoming more widespread at lower elevations (Tab. 1). In addition, a few water samples were collected during the winter seasons 2012 and 2013. Furthermore, a 300 cm-deep snow profile (ca. 2 km far from the glacier, since the glacier area is hardly accessible) was sampled in April 2015, and 6 snow samples were collected at 50-cm intervals for chemical analyses (for each layer, snow density was also measured). A rain collector was installed at the end of July 2015 at ca. 2 km distance from the glacier and sampled when precipitation occurred (5 observations) (Materials and Methods S1.2).

Electrical conductivity (EC) was measured using a Crison - Micro CM 2201. The concentration of major anions (Cl^-, NO_2^--N, NO_3^--N, PO_4^{3-}-P, SO_4^{2-}-S) was determined with a Dionex DX-500 (Dionex Corp., California). Major

cations (Ca^{2+}, Mg^{2+}, K^+, Na^+) were determined by flame atomic absorption spectroscopy using a Perkin Elmer AAnalyst 400 (Perkin-Elmer Inc., Waltham, Massachusetts). Ammonium (NH_4^+-N) was determined spectrophotometrically (U-2000, Hitachi, Tokyo, Japan). DOC and total dissolved nitrogen (TDN) were analysed with a VarioTOC (Elementar, Hanau, Germany). Dissolved organic nitrogen (DON) was estimated from the difference between TDN and dissolved inorganic nitrogen (DIN = NO_3^- + NH_4^+; NO_2^- was always below the detection limit). The quality of chemical analyses was determined by including method blanks and repeated measurements of certified samples. Analytical precision for major anions was <10%, and for major cations was <5%. Analytical precision for DOC and TDN was <2% (Materials and Methods S1.2).

Soil samples were collected close to the water-sampling sites (S1, S2, and S3) (Fig. 1, Tab. 1) during the melting season 2012. Field description of soil profiles was done according to Food and Agriculture Organization-FAO (2006). Soil samples were collected from each genetic horizon (Materials and Methods S1.2). OC and total nitrogen (TN) were analysed by dry combustion with a CN elemental analyzer (CE Instruments NA2100, Rodano, Italy).

2.4 Statistical analysis and loads calculation

From 24 March 2012 to 28 September 2015 sampling of water at W1 site (Fig. 1) was carried out on 41 occasions (Fig. 2), and corresponding daily discharge rates were obtained from the model output at Q1 site. Since the lowermost average modelled discharge during the melting period (April–October) was 0.05 $m^3 s^{-1}$ (year 2014), this threshold was chosen to discriminate between samples collected during low-flow (< 0.05 $m^3 s^{-1}$) and high-flow (≥ 0.05 $m^3 s^{-1}$) periods (Fig. 2, further details in the Results section). This operation was performed in order to investigate the seasonal variations in solute concentrations and their relationships with discharge.

The normality of the data was tested using the Shapiro-Wilk test and data were also tested for homogeneity of variance with the Levene's test (Salerno et al. 2016). Differences in samples between low-flow (18 observations) and high-flow (23 observations) periods were evaluated with one-way analysis of variance (ANOVA), if data were normally distributed. When necessary, data were Log transformed to meet the assumptions of normality. If this failed to improve normality, the Kruskal-Wallis test was applied. Significant differences between water sampling sites along the elevation gradient (26 observations) were determined by means of ANOVA followed by Tukey's multiple comparison test. In case of non-normally-distributed data, nonparametric one-way ANOVA using Wilcoxon (Kruskal-Wallis) scores was performed. All analyses were implemented in the R software (R Core Team, 2018) at a significance level of $p < 0.05$.

DOC and N forms loads from the glacier, except NO_3^--N, were calculated by multiplying the modelled glacier discharge by the mean analyte concentrations due to the lack of dependence of these analytes upon discharge. The uncertainties associated with the mean concentrations were defined as the standard deviations of analyte concentrations,

while the uncertainties associated to the loads also considered the error related to measured *vs.* modelled discharge and were calculated as the root mean square of the errors of the two estimations (Salerno et al. 2016). Given the dependence of NO_3^--N upon discharge, the regression equation was used to calculate daily fluxes. Daily fluxes where then aggregated for the entire investigated period and divided by the analysed years to obtain a mean annual load. The daily load uncertainty was calculated as the root mean square of the regression standard error multiplied by the discharge and the measured *vs.* modelled discharge error. Daily errors were then aggregated for the investigated period divided by the analysed years to obtain a mean annual error.

3 Results

3.1 Meteorological and hydrological conditions

Poly-Hydro model provided rather good depiction of the outlet stream flows from the glacier catchment, both in terms of average flows (*Bias* 2%) and flow variability, as expressed by the Nash-Sutcliffe Efficiency coefficient-NSE = 0.65 (Tab. S2). The modelled hydrographs showed that, after a low winter base flow, glacier discharge generally began to increase during April-May as driven by spring snowmelt, then peaking in June-July (Fig. 2a, 2b). The late summer-autumn decline (until October) was occasionally interrupted by peaks after intense rainfall events (Fig. 2a, 2b). Average modelled discharges during the melting seasons 2012, 2013, 2014, and 2015 were 0.11 (± 0.11), 0.09 (± 0.10), 0.05 (± 0.05), and 0.08 (± 0.08) $m^3\ s^{-1}$, respectively. The overall yearly average stream flow during the four years was estimated at 0.05 (± 0.08) $m^3\ s^{-1}$.

3.2 Discharge-solute relationships, and N and C export

At W1 sampling site, EC was significantly higher during low-flow periods (52.3 ± 24.6 µS cm^{-1}) than during high-flow periods (21.3 ± 9.3 µS cm^{-1}) (Fig. 2c, 3a, Tab. 2). Similar behaviour was found for the dominant major anion (SO_4^{2-}-S) and cation (Ca^{2+}) (Tab. S3). Both ions were significantly higher during low-flow periods (SO_4^{2-}-S = 5.50 ± 3.82 mg L^{-1}; Ca^{2+} = 7.23 ± 4.08 mg L^{-1}) than during high-flow periods (SO_4^{2-}-S = 1.41 ± 1.16 mg L^{-1}; Ca^{2+} = 2.42 ± 1.17 mg L^{-1}) (Fig. 2c, 3b, 3c, Tab. 2). The concentrations of the other ions (i.e. Mg^{2+}, K^+, Na^+, Cl^-) were strongly correlated with EC ($r > 0.78$; except for Cl^-, $r = 0.62$) (Tab. S4); thus EC and the dominant major ions SO_4^{2-}-S and Ca^{2+} were selected as tracers for discussing the geochemical patterns of the Indren Glacier meltwater. Among the N forms, NO_3^--N was the main component, representing a high proportion of TDN (47%), followed by DON (42%) and NH_4^+-N (11%). Similar to EC and major ions, NO_3^--N was significantly higher during low-flow periods (0.30 ± 0.11 mg L^{-1}) than during high-flow periods (0.15 ± 0.07 mg L^{-1}) (Fig.2d, 4a, Tab. 2). In contrast, mean DON concentration did not show statistically significant differences between low-flow (0.20 ± 0.15 mg L^{-1}) and high-flow (0.15 ± 0.14 mg L^{-1}) periods (Fig. 2d, 4b,

187 Tab. 2), as well as NH_4^+-N (not shown). Analogously to DON, mean DOC concentration was similar during low-flow
188 (1.16 ± 0.57) and high-flow (1.15 ± 0.69) periods, not showing any significant difference (Fig. 2d, 4c, Tab. 2). DOC
189 concentration ranged from 0.49 to 3.94 mg L^{-1}, with an average value of 1.16 ± 0.63 mg L^{-1}.

190 Estimated fluxes of TDN, NO_3^--N, DON, NH_4^+-N and DOC were 710 (± 364), 315 (± 183), 300 (± 223), 79 (± 57),
191 and 1,829 (± 994) kg yr^{-1}, respectively. This equated to area-weighted yields (analyte flux divided by the contributing
192 area) for TDN, NO_3^--N, DON, NH_4^+-N, and DOC of 496, 220, 210, 55, and 1,279 kg km^{-2} yr^{-1}, respectively.
193

194 **3.3 N and C in soil, and elevational variations of N forms and DOC in meltwater**

195 Soils displayed different properties according to their different elevations. Organo-mineral horizons enriched in OC
196 were observed in soils located at S2 and S3 sites, deglaciated since the Little Ice Age (LIA), while the few-decade-old
197 till (S1) was depleted (Tab. 3). TN was significantly correlated with OC (r = 0.99) and had an increasing trend with
198 decreasing elevation, showing the highest content in surface A horizons at S2 and S3. S2 and S3 also showed the
199 presence of vegetation, dominated by *Carex curvula* and other species belonging to the *Caricetum curvulae* association.

200 Along the elevation gradient, no significant variations were found in water NO_3^--N, DON, and DOC concentrations
201 (Fig. 5).
202

203 **4 Discussion**

204 **4.2 Loads and possible origin of nitrate and major ions**

205 Nitrate-N mean concentration was consistent with concentrations measured in other glaciated sites and high-elevation
206 surface waters (with varying glacial cover) in Europe (e.g. Tockner et al. 2002; Balestrini et al. 2013; Rogora et al.
207 2013). Nitrogen deposition in the above-mentioned areas was higher (10 to 17 kg N ha^{-1} y^{-1}) than that measured in our
208 study area (6.6 kg N ha^{-1} y^{-1}, as calculated from snow and rain measurements). However, the mean concentrations of
209 NO_3^--N recorded in surface waters were similar, probably because of the lower soil and vegetation cover present in our
210 site, with consequent lower inorganic N retention by soil and vegetation (e.g. Hood et al. 2003). In contrast, NO_3^--N
211 concentration and yield (where reported) were higher than those measured in other glaciated environments across the
212 globe such as in Nepal Himalaya (e.g. Lami et al. 2010; Balestrini et al. 2014), Svalbard (e.g. Wynn et al. 2007),
213 Northern Patagonia (Rogora et al. 2008), and Greenland Ice Sheet (Wadham et al. 2016). In these areas, N
214 concentrations and deposition (in snow and rain, where reported) were generally lower than in our site, suggesting an
215 important role of atmospheric source in N dynamics in different glaciated environments. This is further confirmed by
216 the elevated N concentrations observed in surface waters located in watersheds fed by glaciers such as in the Rocky

Mountains in Colorado (Williams et al. 2007; Baron et al. 2009; Saros et al. 2010), where elevated N deposition (Fenn et al. 2003; Williams et al. 2009) has been reported due intensive industrial and agricultural activity (Baron et al. 2000).

Nitrate-N concentration in a pond without glacier and surrounded by vegetated soil located in the same area of the Indren Glacier (at 2.5 km distance) was ca. three times lower (Magnani et al. 2017) than NO_3^--N measured at W1 site, thus confirming the role of mountain glacier catchments in enriching surface waters in NO_3^- in comparison to snow/groundwater-fed surface waters (Slemmons et al. 2017). Indeed, NO_3^- concentrations in surface waters fed by glacial meltwater have been found to be up to 1−2 orders of magnitude higher than in surface waters fed by snow and groundwater (Saros et al. 2010; Warner et al. 2017), with increasing NO_3^- export from glacial areas that has been reported in the last decades (Barnes et al. 2014). Different explanations have been proposed for the higher NO_3^- content in glacial meltwater, such as reduced contact with watershed soils and vegetation (Brooks et al. 1996), flushing of NO_3^- from microbially active sediments (Baron et al. 2009), and high sublimation and evaporation rates on glaciers leading to concentrated N (Daly and Vania, 2005).

Only NO_3^--N, among the N forms and DOC, was positively correlated to the major ions and negatively correlated to glacier discharge, showing higher concentration in meltwater during low-flow periods (Fig. 2d, 4a, Tab. 2, S4). This occurrence suggests that NO_3^--N derived mainly from subglacial environment. Indeed, during the winter and early melting season (November-April), low discharge in association with higher EC values, and SO_4^{2-}-S and Ca^{2+} concentrations (Fig. 2c, 3) indicate that streamwater chemistry mainly derived from solute-rich subglacial water (winter season) in association with solute-enriched snowmelt due to leaching of ions from the snowpack (early melting season) (Stachnik et al. 2016). Progressive ionic increases from high- to low-flow periods during the melting season (Fig. 2c, 3) suggest that a decreasing ablation rate in the catchment reduced the dilution of solutes by meltwater, resulting in favourable conditions for mineral dissolution beneath the glacier (Stachnik et al. 2016). This is further confirmed by the general behaviour of the major ions, which showed an inverse dependence upon glacier discharge (Tab. S4). In this regard, solute concentrations have been observed to be often inversely related with glacier runoff (Tranter 2006; Yde et al. 2014; Stachnik et al. 2016), with both hydrologic and chemical controls that exist under glaciated conditions (Tranter et al. 2002).

The occurrence of meltwater with longer residence time, routed more slowly through a subglacial distributed drainage system (Tranter et al. 1997; Brown et al. 2006) during low-flow periods is further confirmed by the elevated SO_4^{2-}-S concentration. In particular, S-ratio [SO_4^{2-} / (HCO_3^- + SO_4^{2-})] and Ca-ratio (Ca^{2+} / SO_4^{2-}) (where units of concentrations are expressed in equivalents per litre and HCO_3^- was calculated as the difference between cations and anions since it was not measured in this study) were calculated. The higher S-ratio during low-flow periods (0.68 ± 0.18) with respect to high-flow periods (0.49 ± 0.16) and the lower Ca-ratio during low-flow periods (1.2 ± 0.47) in

comparison to high-flow periods (1.7 ± 0.73) highlighted an enhanced sulphide oxidation and sulphate release. Sulphate can be considered an indicator of distributed type drainage beneath glaciers (Brown et al. 2006; Wadham et al. 2010) and its increase, in most glacial environments, is an effect of increasing residence times and rock/water interaction in subglacial environment (Cooper et al. 2002), where bedrock comminution releases highly reactive sulphide-rich minerals (common in the study area) to meltwater (Tranter et al. 1993). Moreover, high sulphate concentrations in subglacial meltwaters can also be a consequence of microbially-mediated anoxic sulphide oxidation (Tranter et al. 2002). The maximum sulphate concentration that can be generated from sulphide oxidation using oxygen-saturated waters at 0 °C is ca. 400 μeq L^{-1} (Tranter et al. 2002). In our case, sulphate concentrations in bulk runoff up to ca. 1050 μeq L^{-1} during low-flow periods, with a number of samples above 400 μeq L^{-1}, could indicate meltwater drainage from basal regions where additional sulphate contributions may be generated via microbially-mediated anoxic sulphide oxidation (Tranter et al. 2002; Bhatia et al. 2010). Thus, during high-flow periods, most meltwater (including relevant snowmelt contribution) could be intercepted by crevasses and moulins, and drained via major englacial or subglacial conduits with little interaction with subglacial sediments (cf. Hubbard and Nienow, 1997). During low-flow periods, some surface-derived runoff and meltwater produced by basal melting could drain by a more extensive distributed drainage system that allowed more significant water-sediment interaction, with an important contribution of microbially-derived processes to weathering. This hydrological component likely constituted a significant contribution to runoff under recession flow conditions and early in the melt season before the development of major drainage channels (cf. Lafrenière and Sharp 2004).

Microbial activity could contribute to NO_3^- export from the Indren Glacier catchment, thanks to enhanced nitrification from microbial populations in subglacial environment (Wynn et al. 2007; Wadham et al. 2016). Indeed, active microbes have been found in cryospheric settings spanning from arctic to alpine environments (Mader et al. 2006; Williams et al. 2007). Some studies reported that in high-mountain areas also fine sediments under talus deposits are capable of supporting microbial activity, thus contributing in exporting NO_3^- into surface waters (e.g. Williams et al. 1997). However, debris deposits in the W1 site catchment were of minor importance (3.7% of the catchment) and mainly constituted by coarse ablation till, with glacier (64.1%) and steep bedrock (32%) that were the predominant land cover types (Tab. 1). Thus, NO_3^--N contribution from debris deposits outside the glacier body was likely limited. A further evidence of the subglacial origin of NO_3^--N derives from the observation of the NO_3^--N:Cl^- ratios, which were higher in meltwater (2.3) than in rain (1.4) and snow (0.4). Assuming that Cl^- behaved conservatively, then the difference in the NO_3^--N:Cl^- ratio between the glacial meltwater and the other potential N sources can be considered an indication of the effect of catchment processes on NO_3^--N export (Lafrenière and Sharp 2005).

In some occasions, NO_3^--N concentration was found to be high with relatively high discharge towards the end of the melt season. This occurred after heavy rainfall events (e.g. August-September 2012 and 2015, 3 main events) (Fig. 2, 4a). In this case, it is possible that, during rainfall events, water which passed through the glacier flushed water that was potentially stored for some time at the glacier bed, thereby flushing nitrate-rich meltwater from subglacial environment (cf. Theakstone and Knudsen 1996). This is further corroborated by the fact that, during these events, also EC and major ions (especially sulphate) (Fig. 2, 3) increased.

4.2 Loads and possible origin of DOC and DON

The DOC average value (1.16 ± 0.63 mg L^{-1}) in glacial meltwater was approximately three and two times higher than the average global values for mountain glaciers reported by Hood et al. (2015) (0.37 mg L^{-1}) and Li et al. (2018) (0.54 mg L^{-1}), respectively. This resulted in a high yield (1,279 kg km^{-2} yr^{-1}) confirming the high DOC export estimates in the European Alps recently proposed by Li et al. (2018), and far higher than previous average regional estimate for the European Alps (170 kg km^{-2} yr^{-1}) (Singer et al. 2012) and other alpine glaciers (e.g. Roseg and Tschierva glaciers, Switzerland, 360 kg km^{-2} yr^{-1}) (Tockner et al. 2002). This high DOC export could derive from atmospheric deposition (cf. Stibal et al. 2008; Stubbins et al. 2012), considering the location of the Indren Glacier, close to the Po Valley, a European atmospheric pollution hotspot from where air masses can be transported to the NW Alps (Diémoz et al. 2019). DOC concentration in snow in the study area (0.77 ± 0.15 mg L^{-1}) was generally higher than values reported for other glaciated areas, with average values ranging from 0.06 to 0.33 mg L^{-1} (e.g. Stubbins et al. 2012; Spencer et al. 2014; Yan et al. 2016; Musilova et al. 2017). DOC deposition in the Indren Glacier area was 15.5 kg C ha^{-1} y^{-1}, with rain contributing 43% (6.6 kg C ha^{-1} y^{-1}) of the total DOC deposition, which highlighted its relevance in C dynamics in the investigated area. Unfortunately, there are few quantitative studies of OC in atmospheric deposition and even fewer for atmospheric deposition in mountainous environments (Mladenov et al. 2012). However, average DOC concentrations in precipitation in the Turin area and other locations in polluted southern Europe have been found to be between 1.01 and 2.50 mg L^{-1} (Iavorivska et al. 2016), which is consistent with the concentration measured in meltwater and precipitation in this study. Moreover, recent studies reported a number of dust-deposition events in snow- and glacier-covered area of the European Alps (Gabbi et al. 2015; Di Mauro et al. 2019). Thus, a further source of DOC could be linked to dust depositions, since atmospheric aerosol transport is one vector for the delivery of C to alpine areas (Mladenov et al. 2012).

Although DON measurements in glacial meltwater are sparse, DON concentration (0.19 ± 0.14 mg L^{-1}) and yield (210 kg km^{-2} yr^{-1}) in this study were higher than other values reported for few glaciated catchments in Europe (Tockner et al. 2002) and for Greenland Ice Sheet (Wadham et al. 2016), with similar values found in Alaska (Hood and Scott

2008). High N deposition in the study area and site-specific characteristics (e.g. absence of developed soils in the Indren Glacier catchment that could promote mineralisation processes of DON) could explain this occurrence.

In contrast to NO_3^--N and major ions, DON and DOC concentrations were similar during low- and high-flow periods, showing no dependence upon glacier discharge (Fig. 2d, 4b, 4c, Tab. 2, S4). Thus, this occurrence points towards a different origin of DON and DOC with respect to NO_3^--N (and major ions). Previous research suggested that DON and DOC concentrations could derive from different pools of DON (Wadham et al. 2016) and DOC (Bhatia et al. 2013; Spencer et al. 2014) within glaciers.

The acquisition of DON could occur both in surface and basal ecosystems (Wadham et al. 2016), with the presence of a significant N-rich component to dissolved organic matter exported from glacier ecosystems in runoff (Hood et al. 2009; Bhatia et al. 2013). Analogously, DOC could be released from both surface and basal glacial zones. Previous studies have attributed DOC origin in surface waters during the ablation period to DOC leached from wet snow and/or the glacier surface in the supraglacial ecosystems (Stibal et al. 2012a; Spencer et al. 2014). Cryoconite holes were observed to be widely distributed in the ablation area of the Indren Glacier and supraglacial streams transporting organo-mineral material from cryoconite holes to the glacier front were numerous. DOC could originate also at the glacier base, where C is derived from the underlying bedrock, sediments, and ice (Bhatia et al. 2010). Indeed, several authors reported the presence of OC in subglacial environment (Foght et al. 2004; Skidmore et al. 2005; Stibal et al. 2012b), with basal ice showing higher DOC concentrations with respect to surface-englacial ice and cryoconite holes on numerous mountain glaciers (Hood et al. 2015). Interestingly, Colombo et al. (2019) reported that the fluorescence properties of DOC in the Indren proglacial pond were characterised by a high seasonal variability during the melting season 2015. The authors hypothesised that beside an aquatic microbial source of DOC, a source of terrestrially-derived DOC might also exist in the glacier catchment. However, due the fact that W1 site was close to the glacier front and OC in the coarse deposit at S1 site (Fig. 1, Tab. 1) was low (0.14%, Tab. 3), the contribution from the leaching of DOC derived from proglacial detritus areas (cf. McClelland et al. 2014) to meltwater was likely negligible. In addition, developed soils and vegetal material (i.e. plant debris) were absent in the proglacial area. Therefore, it is possible that the re-arrangement and flushing of the subglacial drainage system could cause transient variations in the fluorescence properties of DOC, implying the possible coexistence of sources of terrestrially- and microbially-derived DOC in the subglacial environment (cf. Bhatia et al. 2010). Thus, the OC in the Indren Glacier is probably an amalgamation of supraglacial and subglacial sources (with different microbial and terrestrial origin) (cf. Bhatia et al. 2010; 2013), although further investigations are necessary to properly identify the DOC sources in the Indren Glacier catchment and their fractional contribution to DOC export.

4.2 DOC and N variation along the elevation gradient

Along the elevation gradient, the % of soil cover increased downstream, reaching a value close to 6% at S3 site (Tab. 1), but without any relevant effect on NO_3^--N concentration (Fig. 5a). This could be attributed to the slope steepness and to the fact that the area was recently deglaciated (LIA) with soils showing little development (soil age ca. 170 years), covering a small % of the basin area. A number of studies have demonstrated that, some physical features of the catchment strongly influence the chemical composition of surface water at high elevations (e.g. Clow and Sueker 2000; Balestrini et al. 2013). Balestrini et al. (2013) reported that in some North American and European high-elevation catchments, NO_3^- concentrations in surface waters are inversely related to the areal extensions of developed soils, indicating the fundamental role that the soil biological community plays in the retention and loss of N and therefore the strict connection between soil and waters in mountain remote ecosystems. However, Clow and Sueker (2000) in high-elevation basins in the Colorado Rocky Mountains found how minimal soil development limits chemical weathering and N uptake. Limited soil development in the study area can be explained by the fact that soil evolution, although rather quick in the Alps, could be influenced by frost disturbance and slope instabilities that are able to impede or delay pedogenesis (Haugland 2004).

OC and TN concentrations in soil increased at lower elevation (Tab. 3), without any corresponding increase in DOC and DON in stream water (Fig. 5b, 5c). Several authors reported water DOC increases with increasing distance from the glacier fronts (e.g. Li et al. 2018) and decreasing glaciated areas (e.g. Hood and Scott 2008), due to the loss of terrestrial DOC from unglaciated terrains, implying a strong relationship between soil C pool and DOC export to surface water (Lafrenière and Sharp 2004). Moreover, previous studies reported similar DON yields among catchments with different glacier covers, suggesting that glacial runoff is an important contributor to DON (Hood and Scott 2008). In our site, the higher (although not significant) DOC concentrations at the glacier front and the similar DON concentrations along the elevation gradient point towards the limited effect of soil on water characteristics due to its reduced surface area but, at the same time, underline the importance of the glacier melting in determining N and C dynamics in surface water in this high-elevation, remote environment.

Conclusion

Concentrations and estimated fluxes of N forms and DOC from the high-elevation Indren Glacier catchment were analysed in the period 2012–2015, and concentrations of these analytes in the glacial stream were further investigated along an elevation gradient during 2012–2014. NO_3^--N, as well as EC and major ions, showed a negative relationship with modelled glacier discharge, suggesting a possible subglacial source. DON and DOC were not dependent upon discharge, entailing a potential origin from distinct DON and DOC pools within the glacier. Meltwater concentrations

371 and yields for NO_3^--N (0.21 ± 0.12 mg L^{-1}, 220 kg km^{-2} yr^{-1}), DON (0.19 ± 0.14 mg L^{-1}, 210 kg km^{-2} yr^{-1}), and DOC
372 (1.16 ± 0.63 mg L^{-1}, 1,279 kg km^{-2} yr^{-1}), were among the highest reported for other glaciated areas in the world,
373 probably due to high atmospheric N and C deposition. Minor changes in water NO_3^--N, DON, and DOC concentrations
374 along the elevation gradient suggested a limited effect of soil on water characteristics due to its reduced surface area and
375 little development but, at the same time, underlined the importance of the glacier melting in determining N forms and
376 DOC concentrations in the glacial stream. Further work is needed to improve our understanding of the origin of N
377 forms and DOC in the Indren Glacier meltwater. However, our results contribute to clarifying the little investigated, and
378 yet very important role of fast melting cryospheric features in the Alps, and worldwide, in shaping water quantity and
379 quality downstream under global warming.
380
381 **Acknowledgments**
382 We thank Dr. Eng. Andrea Soncini, Emil Squinobal, Elena Serra, Davide Viglietti, Emanuele Pintaldi and Marco Prati
383 for their help in fieldwork and laboratory activities. We give special thanks to Consorzio di Miglioramento Fondiario di
384 Gressoney (Aosta), Monterosaski, and Monterosa 2000. Fondazione Montagna Sicura is also kindly acknowledged for
385 supporting with ice ablation data. This research was supported by the I CARE Project (Impact of Climate change on
386 Alpine water REsources: the case of Italy and Switzerland) funded under Politecnico5xMille Scheme 2009 and partly
387 by the European Regional Development Fund in Interreg Alpine Space project Links4Soils (ASP399): Caring for Soil-
388 Where Our Roots Grow. Finally, the editor and anonymous reviewers provided valuable feedback and input during the
389 review of this manuscript.
390
391 **References**
392 Balestrini R, Arese C, Freppaz M, Buffagni A (2013) Catchment features controlling nitrogen dynamics in running
393 waters above the tree line (central Italian Alps). Hydrology and Earth System Sciences 17:989–1001
394 Balestrini R, Di Martino N, Van Miegroet H (2006) Nitrogen cycling and mass balance for a forested catchment in the
395 Italian Alps. Biogeochemistry 78:97–123
396 Balestrini R, Polesello S, Sacchi E (2014) Chemistry and isotopic composition of precipitation and surface waters in
397 Khumbu valley (Nepal Himalaya): N dynamics of high elevation basins. Science of the Total Environment 485–
398 486:681–692
399 Barnes RT, Williams MW, Parman JN, Hill K, Caine N (2014) Thawing glacial and permafrost features contribute to
400 nitrogen export from Green Lakes Valley, Colorado Front Range, USA. Biogeochemistry 117:413–430

401 Baron JS, Rueth HM, Wolfe AM, Nydick KR, Allstott EJ, Toby Minear J et al (2000) Ecosystem responses to nitrogen
402 deposition in the Colorado Front Range, Ecosystems 3(4):352–368
403 Baron JS, Schmidt TM, Hartman MD (2009) Climate-induced changes in high elevation stream nitrate dynamics.
404 Global Change Biology 15:1777–1789
405 Baroni C, Bondesan A, Mortara G (2014) Report of the glaciological survey 2013. Geografia Fisica e Dinamica
406 Quaternaria 37:163–227
407 Bhatia M, Das SB, Longnecker K, Charette MA, Kujawinski EB (2010) Molecular characterization of dissolved organic
408 matter associated with the Greenland ice sheet. Geochimica et Cosmochimica Acta 74:3768–3784
409 Bhatia MP, Das SB, Xu L, Charette MA, Wadham JL, Kujawinski EB (2013) Organic carbon export from the
410 Greenland ice sheet. Geochimica et Cosmochimica Acta 109:329–344
411 Bocchiola D, Mihalcea C, Diolaiuti G, Mosconi B, Smiraglia C, Rosso R (2010) Flow prediction in high altitude
412 ungauged catchments: a case study in the Italian Alps (Pantano Basin, Adamello Group). Advances in Water
413 Resources 33:1224–1234
414 Boyd ES, Lange RK, Mitchell AC, Havig JR, Hamilton TL, Lafrenière MJ et al. (2011) Diversity, abundance, and
415 potential activity of a nitrifying and nitrate-reducing microbial assemblages in a subglacial ecosystem. Applied and
416 Environmental Microbiology 77:4778–4787
417 Brighenti S, Tolotti M, Bruno MC, Wharton G, Pusch MT, Bertoldi W (2019) Ecosystem shifts in Alpine streams under
418 glacier retreat and rock glacier thaw: A review. Science of the Total Environment 20(675):542–559
419 Brooks PD, Williams MW, Schmidt SK (1996) Microbial activity under alpine snowpacks, Niwot Ridge, Colorado.
420 Biogeochemistry 32:93–113
421 Brown LE, Hannah DM, Milner AM, Soulsby C, Hodson AJ, Brewer MJ (2006) Water source dynamics in a
422 glacierized alpine river basin (Taillon-Gabietous, French Pyrenees). Water Resources Research 42:W08404,
423 doi:10.1029/2005WR004268
424 CGI-CNR (1961) Catasto dei ghiacciai italiani. CGI (Comitato Glaciologico Italiano)-CNR (Consiglio Nazionale delle
425 Ricerche), vol. 2
426 Clow DW, Sueker JK (2000) Relations between basin characteristics and stream water chemistry in alpine/subalpine
427 basins in Rocky Mountain National Park, Colorado. Water Resources Research 36(1):49–61
428 Colombo N, Giaccone E, Paro L, Buffa G, Fratianni S (2016a) Recent transition from glacial to periglacial environment
429 in a high altitude alpine basin (Sabbione basin, north-western Italian Alps). Preliminary outcomes from a
430 multidisciplinary approach. Geografia Fisica & Dinamica Quaternaria 39(1):21–36

Colombo N, Paro L, Godone D, Fratianni S (2016b) Geomorphology of the Hohsand basin (Western Italian Alps). Journal of Maps 12(5):975–978

Colombo N, Salerno F, Martin M, Malandrino M, Giardino M, Serra E et al. (2019) Influence of permafrost, rock and ice glaciers on chemistry of high-elevation ponds (NW Italian Alps). Science of the Total Environment 685:886–901

Cooper RJ, Wadham JL, Tranter M, Hodgkins R, Peters N (2002) Groundwater hydrochemistry in the active layer of the proglacial zone, Finsterwalderbreen, Svalbard. Journal of Hydrology 269:208–223

Daly GL, Wania F (2005) Organic contaminants in mountains. Environmental Science & Technology 39(2):385–98

Diémoz H, Barnaba F, Magri T, Pession G, Dionisi D, Pittavino S et al. (2019) Transport of Po Valley aerosol pollution to the northwestern Alps – Part 1: Phenomenology. Atmospheric Chemistry and Physics 19:3065–3095

Di Mauro B, Garzonio R, Rossini M, Filippa G, Pogliotti P, Galvagno M et al (2019) Saharan dust events in the European Alps: role in snowmelt and geochemical characterization. The Cryosphere 13:1147–1165

FAO (2006) Guidelines for Soil Description. 4th ed. FAO, Rome

Fellman JB, Hood E, Raymond PA, Hudson J, Bozeman M, Arimitsu M (2015) Evidence for the assimilation of ancient glacier organic carbon in a proglacial stream food web. Limnology and Oceanography 60(4):1118–1128

Fenn ME, Haeuber R, Tonnesen GS, Baron JS, Grossman-Clarke S, Hope D et al. (2003) Nitrogen emissions, deposition and monitoring in the Western United States. BioScience 53:391–403

Foght J, Aislabie J, Turner S, Brown CE, Ryburn J, Saul DJ et al (2004) Culturable bacteria in subglacial sediments and ice from two Southern Hemisphere glaciers. Microbial Ecology 47(4):329–40

Fratianni S, Colombo N, Giaccone E, Acquaotta F, Garzena D, Godone D et al (2015) Effets du changement climatique sur la dégradation du pergélisol dans le N-O de l'Italie : Résultats préliminaires. XXVIIIe Colloque de l'Association Internationale de Climatologie

Gabbi J, Huss M, Bauder A, Cao F, Schwikowski M (2015) The impact of Saharan dust and black carbon on albedo and long-term mass balance of an Alpine glacier. The Cryosphere 9:1385–1400

Giaccone E, Colombo N, Acquaotta F, Paro L, Fratianni S (2015) Climate variations in a high altitude Alpine basin and their effects on a glacial environment (Italian Western Alps). Atmósfera 28(2):117–128

Groppelli B, Soncini A, Bocchiola D, Rosso R (2011) Evaluation of future hydrological cycle under climate change scenarios in a mesoscale Alpine watershed of Italy. Natural Hazards and Earth System Sciences 11:1769–1785

Haugland JE (2004) Formation of patterned ground and fine-scale soil development within two late Holocene glacial chronosequences: Jotunheimen, Norway. Geomorphology 61:287–301

Hood E, Battin TJ, Fellman J, O'Neel S, Spencer RGM (2015) Storage and release of organic carbon from glaciers and ice sheets. Nature Geoscience 8(2):91–96

462 Hood E, Fellman J, Spencer RGM, Hernes PJ, Edwards R, D'Amore D et al (2009) Glaciers as a source of ancient and
463 labile organic matter to the marine environment. Nature 462:1044–1047
464 Hood E, Scott D (2008) Riverine organic matter and nutrients in southeast Alaska affected by glacial coverage. Nature
465 Geoscience 1:583–587
466 Hood E, Williams MW, Caine N (2003) Landscape controls on organic and inorganic nitrogen leaching across an
467 alpine/subalpine ecotone, Green Lakes Valley, Colorado Front Range. Ecosystems 6(1):31-45
468 Hubbard B and Nienow P (1997) Alpine subglacial hydrology. Quaternary Science Reviews 16:939–955.
469 Iavorivska L, Boyer EW, DeWalle DR (2016) Atmospheric deposition of organic carbon via precipitation. Atmospheric
470 Environment 146:153–163
471 Lafrenière MJ, Sharp MJ (2004) The concentration and fluorescence of dissolved organic carbon (DOC) in glacial and
472 non-glacial catchments: interpreting hydrological flow routing and DOC sources. Arctic, Antarctic, and Alpine
473 Research 36(2):156–165
474 Lafrenière MJ, Sharp MJ (2005) A comparison of solute fluxes and sources from glacial and non-glacial catchments
475 over contrasting melt seasons. Hydrological Processes 19:2991–3012
476 Lami A, Marchetto A, Musazzi S, Salerno F, Tartari G, Guilizzoni P et al (2010) Chemical and biological response of
477 two small lakes in the Khumbu Valley, Himalayas (Nepal) to short-term variability and climatic change as detected
478 by long-term monitoring and paleolimnological methods. Hydrobiologia 648:189−205
479 Li X, Ding Y, Xu J, He X, Han T, Kang S et al (2018) Importance of mountain glaciers as a source of dissolved organic
480 carbon. Journal of Geophysical Research: Earth Surface 123:2123–2134
481 Mader HM, Pettitt ME, Wadham JL, Wolff EW, Parkes RJ (2006) Subsurface ice as a microbial habitat Geology 34:
482 169–172
483 Maggioni M, Freppaz M, Piccini P, Williams M, Zanini E (2009) Snow cover effects on glacier ice surface temperature.
484 Arctic, Antarctic, and Alpine Research 41(3):323–329
485 Magnani A, Viglietti D, Balestrini R, Williams MW, Freppaz M (2017) Contribution of deeper soil horizons to N and C
486 cycling during the snow-free season in alpine tundra, NW Italy. Catena 155:75–85
487 McClelland JW, Townsend-Small A, Holmes RM, Pan F, Stieglitz M, Khosh M et al (2014) River export of nutrients
488 and organic matter from the North Slope of Alaska to the Beaufort Sea. Water Resources Research 50:1823–1839
489 Milner AM, Khamis K, Battin TJ, Brittain JE, Barrand NE, Füreder L et al (2017) Glacier shrinkage driving global
490 changes in downstream systems. Proceedings of the National Academy of Sciences of the United States of America
491 114(37):9770–9778

492 Mladenov N, Williams MW, Schmidt SK, Cawley K (2012) Atmospheric deposition as a source of carbon and nutrients
493 to an alpine catchment of the Colorado Rocky Mountains. Biogeosciences 9:3337–3355
494 Musilova M, Tranter M, Wadham J, Telling J, Tedstone J, Anesio AM (2017) Microbially driven export of labile
495 organic carbon from the Greenland ice sheet. Nature Geoscience 10(5):360–365
496 Piccini P (2007) Ghiacciai in Valsesia. Edizioni Società Meteorologica Subalpina, Bussoleno
497 R Core Team (2018) R: A language and environment for statistical computing. R Foundation for Statistical Computing,
498 Vienna, Austria, URL https://www.R-project.org/
499 Rogora M, Colombo L, Lepori F, Marchetto A, Steingruber S, Tornimbeni O (2013) Thirty years of chemical changes
500 in alpine acid-sensitive lakes in the Alps. Water, Air, & Soil Pollution 224:1746, doi.org/10.1007/s11270-013-1746-
501 3
502 Rogora M, Massaferro J, Marchetto A, Tartari G, Mosello R (2008) The water chemistry of some shallow lakes in
503 Northern Patagonia and their nitrogen status in comparison with remote lakes in different regions of the globe.
504 Journal of Limnology 67(2):75–86
505 Salerno F, Thakuri S, Guyennon N, Viviano G, Tartari G (2016) Glacier melting and precipitation trends detected by
506 surface area changes in Himalayan ponds. The Cryosphere 10(4):1433–1448
507 Saros JE, Rose KC, Clow DW, Stephens VC, Nurse AB, Arnett HA et al. (2010) Melting alpine glaciers enrich high-
508 elevation lakes with reactive nitrogen. Environmental Science & Technology 44(13):4891–96
509 Singer GA, Fasching C, Wilhelm L, Niggemann J, Steier P, Dittmar T et al (2012) Biogeochemically diverse organic
510 matter in Alpine glaciers and its downstream fate. Nature Geoscience 5:710–714
511 Singh VB, Ramanathan AL, Pottakkal JG, Sharma P, Linda A, Azam MF et al (2012) Chemical characterisation of
512 meltwater draining from Gangotri Glacier, Garhwal Himalaya, India. Journal of Earth System Science 121(3):625-
513 636
514 Skidmore M, Anderson SP, Sharp MJ, Foght J, Lanoil BD (2005) Comparison of microbial community compositions of
515 two subglacial environments reveals a possible role for microbes in chemical weathering processes in an alpine
516 catchment. Applied and Environmental Microbiology 71(11):6986–6997
517 Slemmons KE, Rodgers ML, Stone JR, Saros JE (2017) Nitrogen subsidies in glacial meltwaters have altered
518 planktonic diatom communities in lakes of the US Rocky Mountains for at least a century. Hydrobiologia
519 800(1):129–144
520 Slemmons KE, Saros JE (2012) Implications of nitrogen-rich glacial meltwater for phytoplankton diversity and
521 productivity in alpine lakes. Limnology and Oceanography 57(6):1651–63

522 Slemmons KE, Saros JE, Simon K (2013) The influence of glacial meltwater on alpine aquatic ecosystems: A review.
523 Environmental Sciences: Processes and Impacts 15:1794–1806
524 Soncini A, Bocchiola D, Azzoni RS, Diolaiuti GA (2017) A methodology for monitoring and modeling of high altitude
525 Alpine catchments. Progress in Physical Geography 41(4):393–420
526 Soncini A, Bocchiola D, Confortola G, Bianchi A, Rosso R, Mayer C et al (2015) Future hydrological regimes in the
527 upper Indus basin: a case study from a high altitude glacierized catchment. Journal of Hydrometeorology 16(1):306–
528 326
529 Spencer RGM, Vermilyea A, Fellman J, Raymond P, Stubbins A, Scott D et al (2014) Seasonal variability of organic
530 matter composition in an Alaskan glacier outflow: Insights into glacier carbon sources. Environmental Research
531 Letters 9(5):055005, doi.org/10.1088/1748-9326/9/5/055005
532 Stachnik L, Majchrowska E, Yde JC, Nawrot AP, Cichała-Kamrowska K, Ignatiuk D et al (2016) Chemical denudation
533 and the role of sulfide oxidation at Werenskioldbreen, Svalbard. Journal of Hydrology 538:177–193
534 Stahl K, Moore RD, Shea JM, Hutchinson D, Cannon AJ (2008) Coupled modelling of glacier and streamflow response
535 to future climate scenarios. Water Resources Research 44(2):W02422, doi: 10.1029/2007WR005956
536 Stibal M, Šabacká M, Žárský J (2012a) Biological processes on glacier and ice sheet surfaces. Nature Geoscience
537 5(11):771–774
538 Stibal M, Tranter M, Benning LG, Řehák J (2008) Microbial primary production on an Arctic glacier is insignificant in
539 comparison with allochthonous organic carbon input. Environmental Microbiology 10:2172–2178
540 Stibal M, Wadham JL, Lis GP, Telling J, Pancost RD, Ashley Dubnick et al (2012b) Methanogenic potential of Arctic
541 and Antarctic subglacial environments with contrasting organic carbon sources. Global Change Biology 18:3332–
542 3345
543 Stubbins A, Hood E, Raymond PA, Aiken GR, Sleighter RL, Hernes PJ et al (2012) Anthropogenic aerosols as a source
544 of ancient dissolved organic matter in glaciers. Nature Geoscience 5(3):198–201
545 Theakstone WH, Knudsen NT (1996) Isotopic and ionic variations in glacier river water during three contrasting
546 ablation seasons. Hydrological Processes 10:523–539
547 Tockner K, Malard F, Uehlinger U, Ward JV (2002) Nutrients and organic matter in a glacial river–floodplain system
548 (Val Roseg, Switzerland). Limnology and Oceanography 47(1):266–277
549 Tranter M (2006) Glacial chemical weathering, runoff composition and solute fluxes. In Knight PG (ed.), Glacier
550 Science and Environmental Change, Wiley-Blackwell, 71–75
551 Tranter M, Brown GH, Raiswell R, Sharp M, Gurnell A (1993) A conceptual model of solute acquisition by Alpine
552 glacial meltwaters. Journal of Glaciology 39:573–581

553 Tranter M, Sharp MJ, Brown GH, Willis IC, Hubbard BP, Nielsen MK et al (1997) Variability in the chemical
554 composition of in situ subglacial meltwaters. Hydrological Processes 11:59–77
555 Tranter M, Sharp MJ, Lamb HR, Brown GH, Hubbard BP, Willis IC (2002) Geochemical weathering at the bed of Haut
556 Glacier d'Arolla. Switzerland - a new model. Hydrological Processes 16:959–993
557 Viviroli D, Archer DR, Buytaert W, Fowler HJ, Greenwood GB, Hamlet AF et al (2011) Climate change and mountain
558 water resources: overview and recommendations for research, management and policy. Hydrology and Earth System
559 Sciences 15:471–504
560 Wadham JL, Hawkings J, Telling J, Chandler D, Alcock J, O'Donnell E et al (2016) Sources, cycling and export of
561 nitrogen on the Greenland Ice Sheet. Biogeosciences 13:6339–6352
562 Wadham JL, Tranter M, Hodson AJ, Hodgkins R, Bottrell S, Cooper R et al (2010) Hydro-biogeochemical coupling
563 beneath a large polythermal Arctic glacier: Implications for subice sheet biogeochemistry. Journal of Geophysical
564 Research 115:F04017, doi.org/10.1029/2009JF001602
565 Warner KA, Saros JE, Simon KS (2017) Nitrogen subsidies in glacial meltwater: implications for high elevation aquatic
566 chains. Water Resources Research 53(11):9791–9806
567 Williams MW, Davinroy T, Brooks PD (1997) Organic and inorganic nitrogen pools in talus fields and subtalus water,
568 Green Lakes Valley, Colorado Front Range. Hydrological Processes 11:1747–1760
569 Williams MW, Knauf M, Cory R, Caine N, Liu N (2007) Nitrate content and potential microbial signature of rock
570 glacier outflow, Colorado Front Range. Earth Surface Processes and Landforms 32:1032–1047
571 Williams MW, Seibold C, Chowanski K (2009) Storage and release of solutes from a subalpine seasonal snowpack: soil
572 and stream water response, Niwot Ridge, Colorado. Biogeochemistry 95:77–94
573 Wynn PM, Hodson AJ, Heaton THE, Chenery SR (2007) Nitrate production beneath a high arctic glacier, Svalbard.
574 Chemical Geology 244:88–102
575 Yan F, Kang S, Li C, Zhang Y, Qin X, Li Y (2016) Concentration, sources and light absorption characteristics of
576 dissolved organic carbon on a medium-sized valley glacier, northern Tibetan Plateau. The Cryosphere 10:2611–
577 2621
578 Yde JC, Tvis Knudsen N, Hasholt B, Mikkelsen AB (2014) Meltwater chemistry and solute export from a Greenland
579 Ice Sheet catchment, Watson River, West Greenland. Journal of Hydrology 519:2165–2179

Figures and tables

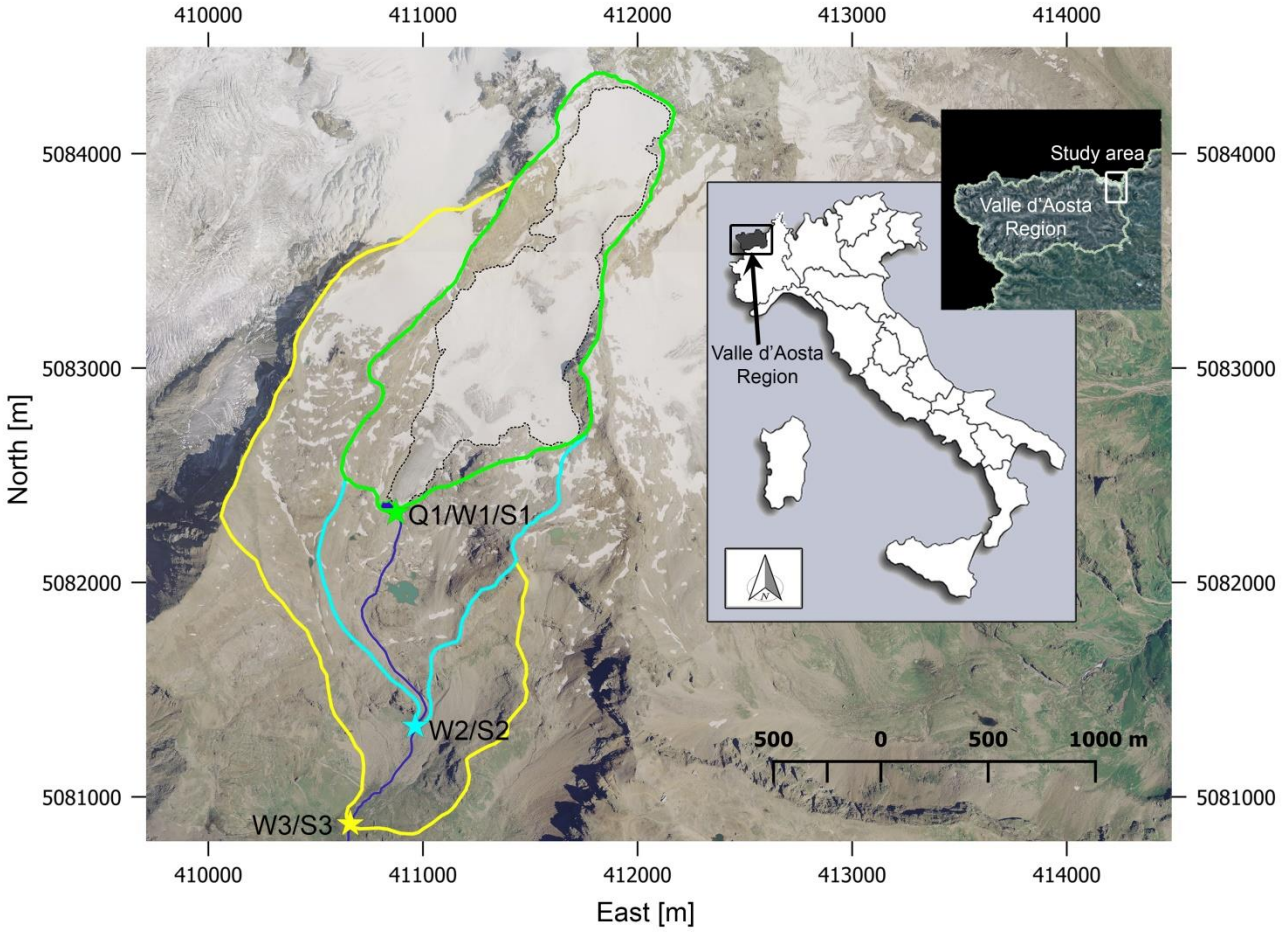

Fig. 1 Location of the study area in Italy and in the Valle d'Aosta Region (www.pcn.minambiente.it), and aerial overview of the study area (orthoimage year 2006) (coordinate system WGS84 / UTM 32N). Black dotted polygon indicates the glacier surface. Stars refer to sampling sites along the glacial stream. Polygons refer to sampling site basins: green - Q1/W1/S1, cyan - W2/S2, and yellow - W3/S3. Details of sampling sites are reported in Table 1.

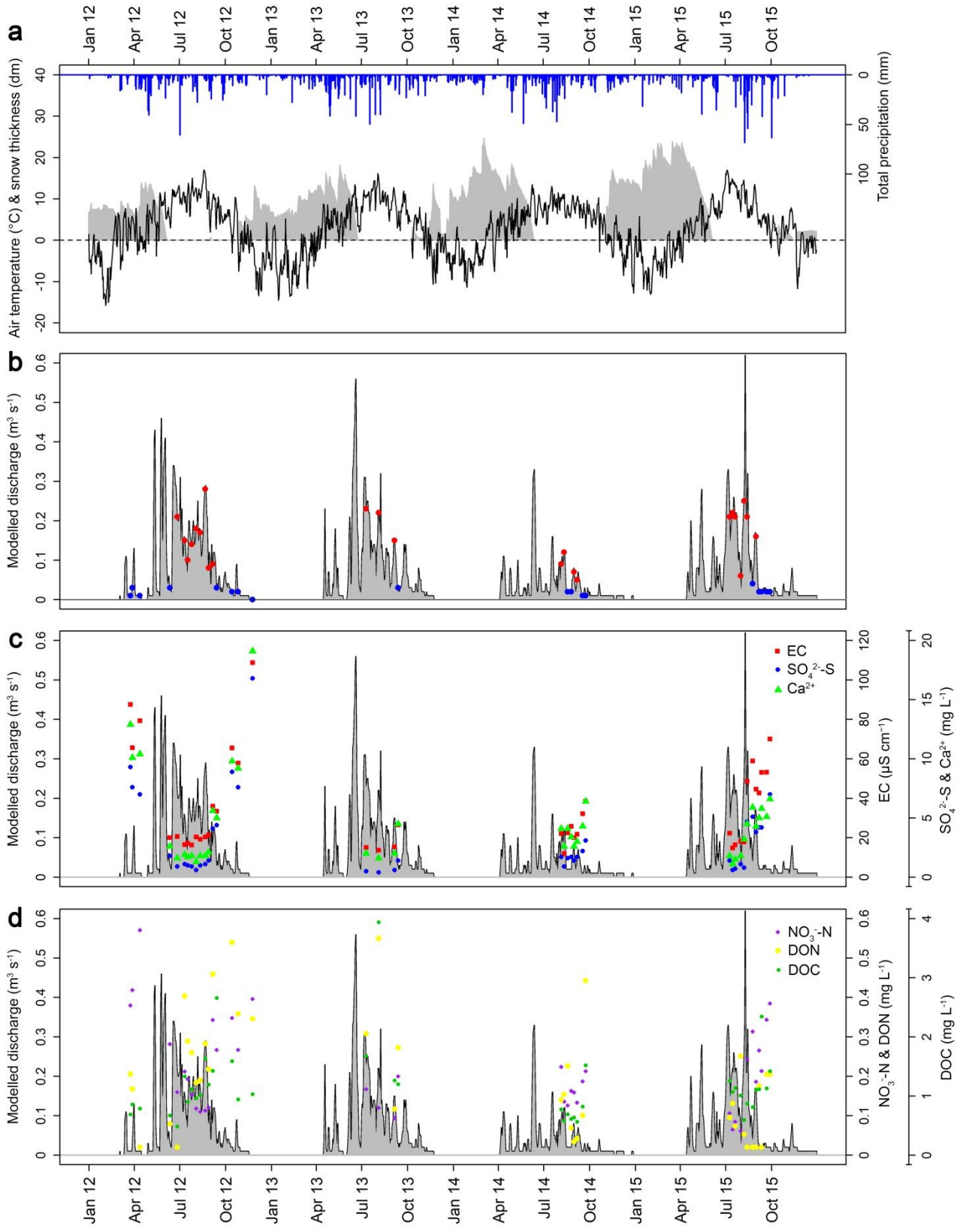

586

587 Fig. 2 (a) Mean daily air temperature (black line), snow thickness (grey polygons), and total precipitation (blue
588 histograms) (Gabiet AWS, Tab. S1). (b) Modelled glacier discharge at Q1 site (grey polygons with black contour). Blue
589 and red dots indicate the sampling dates during low- and high-flow periods, respectively. Time series of relation
590 between modelled glacier discharge and (c) EC / SO_4^{2-}-S / Ca^{2+}, and (d) NO_3^--N / DON / DOC.

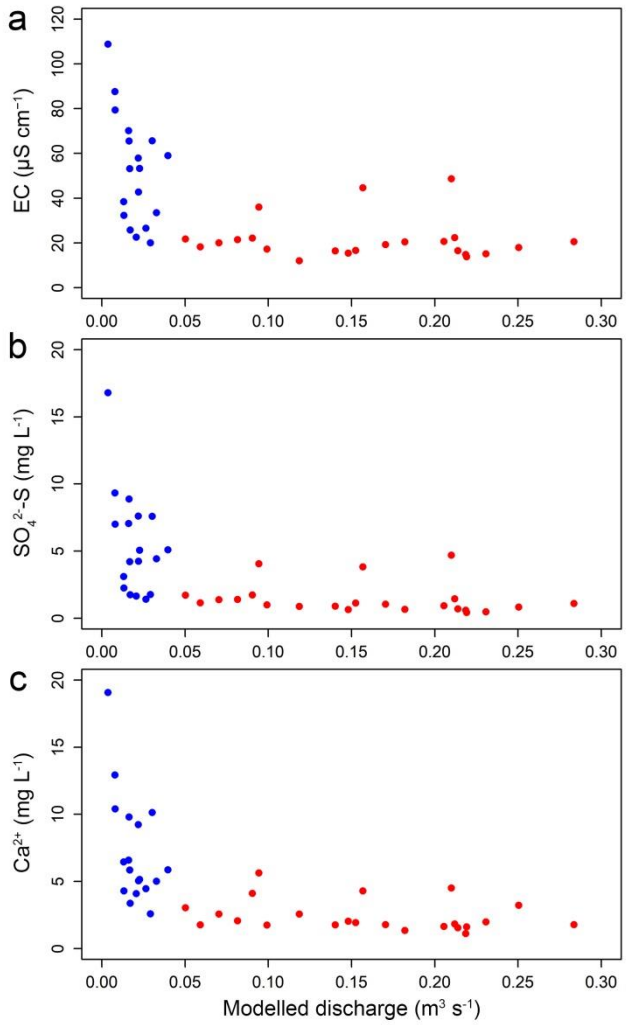

591

592 Fig. 3 Modelled glacier discharge versus (a) EC, and (b) SO_4^{2-}-S and (c) Ca^{2+} concentrations. Blue and red dots indicate

593 the sampling dates during low- and high-flow periods, respectively.

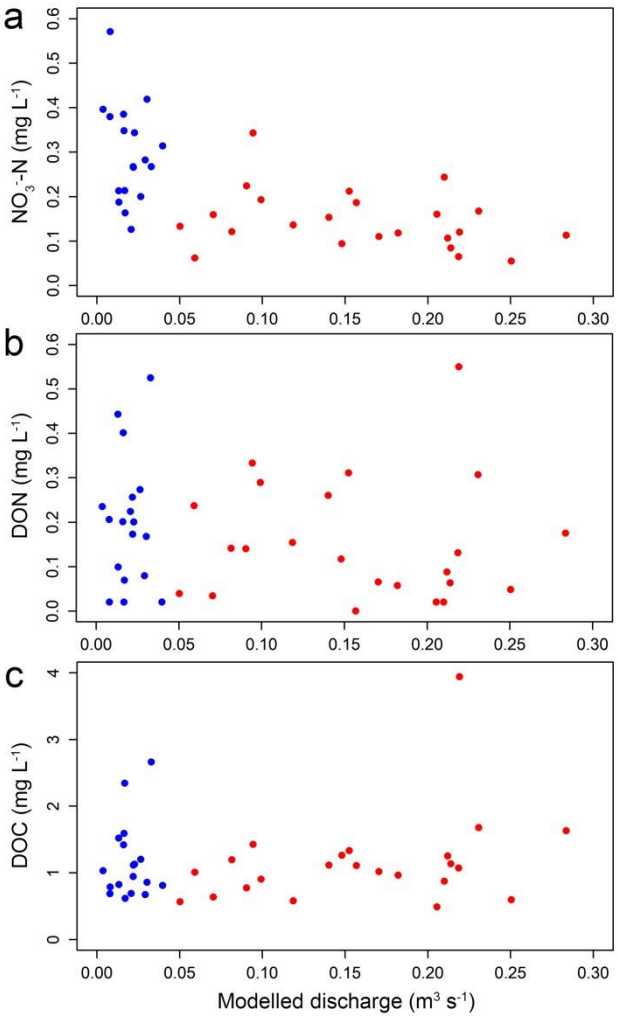

Fig. 4 Modelled glacier discharge versus (a) NO_3^--N, (b) DON, and (c) DOC concentrations. Blue and red dots indicate the sampling dates during low- and high-flow periods, respectively.

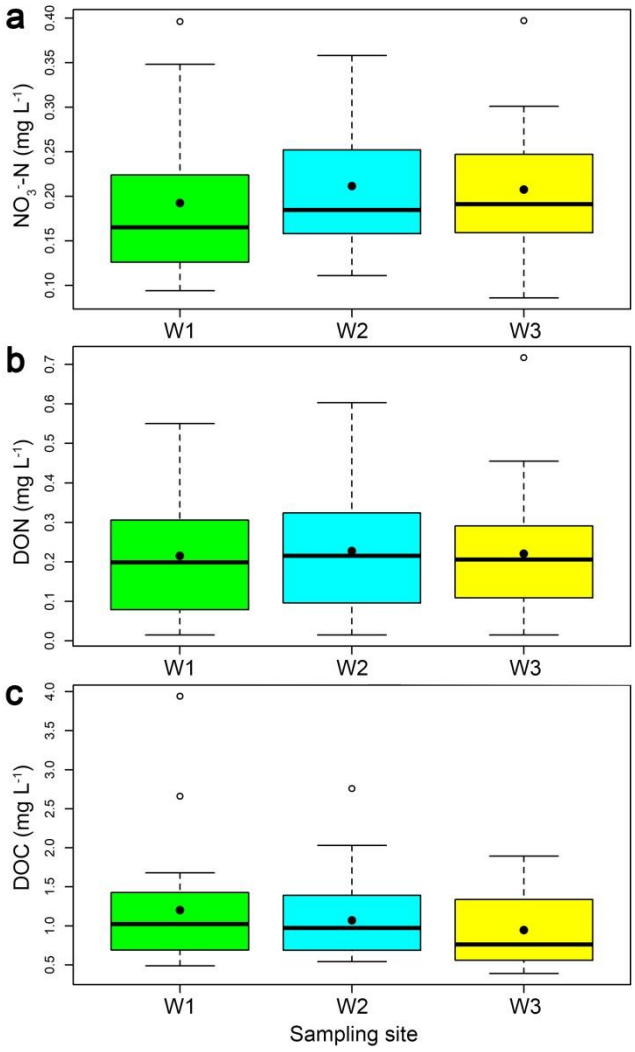

597

598 Fig. 5 (a) NO_3^--N, (b) DON, and (c) DOC concentrations in the glacial stream along the elevation gradient (n = 26).
599 Black dots indicate the mean. Sampling site locations and relative basins are reported in Figure 1. Further details about
600 the sampling sites are reported in Table 1.

Parameter	Indren Glacier	Parameter	Q1/W1/S1 sampling site	W2/S2 sampling site	W3/S3 sampling site
Elevation range (m a.s.l.)	3083 – 4081	Elevation (m a.s.l.)	3083	2695	2605
Area, year 2006 (km^2)	0.92	Basin area (km^2)	1.43	2.12	3.59
Length / width (m)	2310 / 740	Distance from the glacier (km)	-	1	1.4
		Basin land cover	Glacier: 64.1%	Glacier: 43.1%	Glacier: 31%
			Bedrock: 32%	Bedrock: 38.9%	Bedrock: 29.2%
			Coarse sediment: 3.7%	Coarse sediment: 16.9%	Coarse sediment: 33.7%
			Soil: 0%	Soil: 0.4%	Soil: 5.6%
			Water surface: 0.2%	Water surface: 0.7%	Water surface: 0.4%

601 Table 1 Morphometric characteristics of the Indren Glacier, and morphometric and land cover characteristics of the sampling sites. The relevant maps are reported in Figure 1.

Parameter	Low-flow period	High-flow period
EC (µS cm^{-1}, 20 °C)	52.3 ± 24.6	21.3 ± 9.3
SO_4^{2-}-S (mg L^{-1})	5.50 ± 3.82	1.41 ± 1.16
Ca^{2+} (mg L^{-1})	7.23 ± 4.08	2.42 ± 1.17
NO_3^--N (mg L^{-1})	0.30 ± 0.11	0.15 ± 0.07
DON (mg L^{-1})	0.20 ± 0.15	0.15 ± 0.14
DOC (mg L^{-1})	1.16 ± 0.57	1.15 ± 0.69

602 Table 2 EC, and SO_4^{2-}-S, Ca^{2+}, NO_3^--N, DON, and DOC concentrations during low- and high-flow periods. Mean ±
603 standard deviation are reported.

Sampling site	Horizon	Depth (cm)	OC (%)	TN (%)
S1	C	0-10	0.14	0.01
S2	A1	0-2	3.86	0.27
	A2	2-10	0.96	0.07
	AC	10-20+	0.35	0.02
S3	A	0-2	5.52	0.37
	CA	2-7	0.87	0.05
	2CB	7-20+	0.22	0.02

Table 3 Soil characteristics across the elevation gradient. Locations and details of sampling sites are reported in Figure 1 and Table 1.